VI International Conference on Particle-based Methods – Fundamentals and Applications
PARTICLES 2019
E. Oñate, M. Bischoff, D.R.J. Owen P. Wriggers, , & T. Zohdi (Eds)

WCSPH FOR MODELLING MULTIPHASE FLOWS AND NATURAL HAZARDS

S. MANENTI

Dipartimento di Ingegneria Civile e Architettura (DICAr), University of Pavia
Via Ferrata, 3 – 27100 Pavia (Italy)
sauro.manenti@unipv.it - http://civrisk.unipv.it/teaching-staff/sauro-manenti/

Key words: Multiphase, WCSPH, high density ratio, limiting viscosity, non-Newtonian fluid, natural hazards.

Abstract. Among the numerous types of meshless particle methods, SPH is successfully applied to simulate complex multiphase flows with impact involving fluids with high-density ratio as well as non-Newtonian fluids. These problems are concern in the applied engineering dealing with water related natural hazards, such as landslide induced tsunami in artificial reservoir, intense rainfall induced shallow landslides. This contribution aims at providing an overview on the recent applications of the standard weakly compressible WCSPH for modelling these kinds of multiphase flows. The relevant aspects related with the interface treatment and numerical stability in high density multiphase flow will be discussed. Advanced modelling aspects connected with the SPH simulation of non-Newtonian fast dense granular flows and the interaction with pore water. The aspect of tuning model parameters is discussed.

1 INTRODUCTION

Multiphase flows are involved in several problems of practical interests and in many fields of the hydraulic engineering (Guandalini et al. 2015, Todeschini et al. 2019). Among these, the analysis of natural hazardous events related to water represents an important category (Manenti et al. 2018; Manenti et al. subm.). These problems are frequently characterized by fast dynamics, large deformation, flow impact and possibly large density ratio. These peculiar features of the multiphase flow may be difficult to handle from numerical point of view. This is especially the case of multiphase flows where high-density ratio between the phases can cause numerical instability (Monaghan & Ashkan 2013; Grenier et al. 2009; Hu & Adams 2007; Colagrossi & Landrini 2003). Other relevant issues in the numerical modelling of complex multiphase problems of practical interests are: (*i*) stochastic nature of modelling parameters influencing the model response (Manenti et al. 2016), and (*ii*) the large amount of computational time and resources required by complex problems and time step limitation when considering viscous non-Newtonian fluids (Manenti et al. 2018; Guandalini et al. 2012). Therefore fast-running reliable numerical models are strongly desirable, especially for application to multi-disciplinary decision support systems for natural hazard risk reduction and management where several scenarios should be explored to account for inherent uncertainty affecting influential model parameters (Newman et al. 2017).

In this paper will be discussed some modelling approaches for handling the above-mentioned issues in the WCSPH simulation of multiphase flows involved in natural hazards.

2 MODEL DESCRIPTION

In this section will be illustrated two different WCSPH models for the analysis of multiphase flows.

In section 2.1 are shown the analytical details of a relatively simple and novel approach based on standard weakly compressible SPH for simulating free-surface multiphase flows with high-density ratio involving violent impact (Manenti 2018). The proposed approach, which is relatively simple to implement, allows keeping sharp interfaces between the two phases and permits to overcome instability problems affecting standard SPH formulation in these kind of applications.

In section 2.2 is illustrated the FOSS code SPHERA v.9.0.0 (RSE SpA) (Amicarelli et al. subm.) that is based on the standard WCSPH formulation featuring a mixture model for the analysis of dense granular flows consistent with the Kinetic Theory of Granular Flow (KTGF) (Amicarelli et al. 2017). A numerical parameter, so-called limiting viscosity, has been subsequently introduced in the reference model of Amicarelli et al. (2017) as an appropriate means to reduce computational time in those kind of multiphase flows involving a viscous non-Newtonian fluid, as the case of landslide post-failure dynamics (Manenti et al. 2018).

2.1 Novel WCSPH for high-density ratio two-phase flow

In the following are described the governing equations of an alternative SPH model that derives from the discretized balance equations of fluid motion described in Monaghan (1994) which were defined as "standard" formulation in Colagrossi & Landrini (2003). Even if multiphase flows can be simulated following standard SPH (Manenti et al. 2012), serious numerical instability at the interface arises when the density ratio between involved phases increases at some order of magnitude. The principal causes of this instability was investigated in Manenti (2018) and were due mainly to the discontinuity of density across the interface. Adopting the formalism introduced in that work, the mass and momentum balance equations in the standard SPH formulation can be conveniently formulated, as explained in the following, substituting the density ρ_i of a given fluid particle at the point $\mathbf{x}_i$, which becomes discontinuous across the interface, with the inverse of the its particle volume V_i:

$$\rho_i = m_i \frac{1}{V_i} = m_i \varpi_i \tag{1}$$

The symbol ϖ_i in Eq. (1) is used to denote the inverse of the particle volume (or number density) which is referred to as the specific volume, according to the nomenclature adopted in Hu and Adams (2007). Note that, as the specific volume is continuous across the interface, the particle's mass is discontinuous. The particle mass m_i is assumed as constant.

Thus the differential balance equations for the mass and momentum ($\mathbf{v}$ velocity vector, $\mathbf{g}$ gravitational acceleration, p pressure) of a slightly compressible inviscid fluid can be written:

$$\begin{aligned} \frac{D\varpi_i}{Dt} &= -\varpi_i \nabla \cdot \mathbf{v}_i \\ \frac{D\mathbf{v}_i}{Dt} &= -\frac{1}{m_i \varpi_i} \nabla p_i + \mathbf{g} \end{aligned} \tag{2}$$

The discretized form of the mass and momentum balance Eqs. (2) can be obtained by applying the standard SPH approximation principles after the following simple mathematical manipulations:

$$\frac{D\varpi_i}{Dt} = -\left[\nabla\left(\varpi\,\mathbf{v}\right)_i - \mathbf{v}_i \cdot \nabla\varpi_i\right] \tag{3}$$

$$\frac{D\mathbf{v}_i}{Dt} = -\frac{1}{m_i}\left[\frac{p_i}{\varpi_i^2}\nabla\varpi_i + \nabla\left(\frac{p_i}{\varpi_i}\right)\right] + \mathbf{g} \tag{4}$$

If the support of the kernel is not truncated (as occurs when intersecting the fluid free surface), a useful relation can be derived for the derivative of a function f (Liu & Liu, 2003). Considers the following integral kernel approximation of the quantity ∇f evaluated at the i-th point of the continuum domain Ω:

$$\nabla f_i = \int_{\Omega} \nabla_j f_j \, W_{ij} \, d\Omega \tag{5}$$

In the Eq. (5), the gradient on the left side member is calculated at particle i (subscript i is omitted for nabla operator), while it is evaluated at particle j on the right-hand member (i.e. ∇_j). Taking into account the following identity:

$$\nabla_j f_j \, W_{ij} = \nabla_j \left[f_j \, W_{ij}\right] - f_j \, \nabla_j W_{ij} \tag{6}$$

the Eq. (5) can be rewritten in the following manner if the Gauss divergence theorem is applied at the first integral on the right side member:

$$\nabla f_i = \int_{\partial\Omega} f_j \, W_{ij} \cdot \mathbf{n} \, ds - \int_{\Omega} f_j \, \nabla_j \, W_{ij} \, d\Omega \tag{7}$$

Because the kernel W_{ij} is a central function of the relative distance between particles i and j, it can be easily demonstrated that the kernel gradient ∇W_{ij} evaluated at particle i has opposite sign with respect to the kernel gradient $\nabla_j W_{ij}$ at particle j. In addition, if the kernel compact support (which is function of the smoothing length h) is entirely contained in the domain Ω then the first integral on the right-hand side of Eq. (7) vanishes since it is evaluated on the frontiers $\partial\Omega$ of Ω and the kernel function is zero outside its support by definition. For the above-mentioned reasons Eq. (7) becomes:

$$\nabla f_i = \int_{\Omega} f_j \, \nabla W_{ij} \, d\Omega \tag{8}$$

As the discrete element volume is ϖ_j^{-1}, the particle approximation of Eq. (8) is given by:

$$\nabla f_i = \sum_{j=1}^{Ni} \frac{1}{\varpi_j} f_j \cdot \nabla W_{ij} \tag{9}$$

Taking into account Eq. (9) with f equal to $(\varpi_i \, \mathbf{v}_i)$ and ϖ_i respectively, the mass balance in

Eq. (3) can be discretized as follows:

$$\frac{D\varpi_i}{Dt} = -\sum_{j=1}^{Ni} \nabla\left(\mathbf{v}_j - \mathbf{v}_i\right) \cdot \nabla W_{ij} \tag{10}$$

In a similar fashion, by replacing f into Eq. (9) with ϖ_i and (p_i / ϖ_i) respectively, from Eq. (4) can be obtained the discretized momentum balance equation:

$$\frac{D\mathbf{v}_i}{Dt} = -\frac{1}{m_i} \sum_{j=1}^{Ni} \left(\frac{p_i}{\varpi_i^2} + \frac{p_j}{\varpi_j^2} \right) \nabla W_{ij} + \mathbf{g} \tag{11}$$

In Eq. (11) the artificial viscosity term Π_{ij} is introduced to assure numerical stability and to keep interface sharply defined. This term derives from the artificial viscosity of Monaghan (1994) following proper adaptation to be consistent with the model formulation that adopts specific volume as independent variable instead of the density (Manenti 2018).

The discretized governing Eqs. (10) and (11) provide the following advantages when dealing with multiphase flows with large density ratio: (*i*) each phase is not treated as a boundary condition for the other and all neighboring particles in the interaction domain of an interface particle are included into its neighbor's list, regardless of the phase they belong to; (*ii*) kernel truncation is avoided, requiring no need for numerical correctives to improve the accuracy at the interface; (*iii*) no kind of cohesion force is required for eliminating particle penetration between heterogeneous phases at the interface; (*iv*) the algorithm is relatively simple to implement and reduce computational effort.

This model has recently been tested on air-water rapidly varied flow with impact showing reliable accuracy, especially if compared with its relative simplicity (Manenti 2018). Section 3.1 shows the results for another application to the rise of an air bubble in still water.

2.2 WCSPH with limiting viscosity

The numerical investigation of complex 3D problems of practical interest frequently requires the discretization of large domains with a high resolution. This lead to an exponential growth of required computational time and involved resources, especially in the case of SPH method, which could be much more expensive than traditional grid-based methods. A help comes from the recent increase of the parallel computational power of the hardware, especially in the branch of Graphics Processing Units (GPUs). Anyway, GPUs based computations require that the models are implemented using High Performance Computing (HPC) techniques to take advantage of the power of current hardware (Domínguez et al. 2013).

As explained in the following, a simple strategy may be applied in those cases involving viscous non-Newtonian fluid to carry out code optimization for reducing significantly the computational time while preserving suitable degree of accuracy.

The FOSS code SPHERA v.9.0.0 (Amicarelli et al. subm.) implements a WCSPH formulation of mixture model for the analysis of dense granular flows consistent with the KTGF (Amicarelli et al. 2017). This model has been successfully applied to the analysis of rapid multiphase flow involving the interaction of fast landslide with stored water (Manenti et

al. 2018). Post-failure landslide dynamics is simulated by assuming a non-Newtonian rheological model for the slide mass that mimics pseudo-plastic behavior. Time step reduction occurs when shear rate approaches zero and the apparent viscosity approaches higher values. In order to reduce computational time a numerical parameter is introduced which is referred to as limiting viscosity μ_0. Following the experimental behavior exhibited by high polymer solutions, the transition from frictional regime (i.e. solid particle in motion) to the elastic-plastic regime (i.e. solid particle at rest) occurs with an almost constant value of the apparent viscosity which is set equal to μ_0. This allows keep control of the growth of viscosity at very low shear rate, thus reducing computational time when the stability condition for the explicit integration scheme is dominated by viscous criterion.

This approach has been successfully tested on a laboratory experiment simulating, along a representative transversal section, the 2D run-out of the Vajont landslide and its interaction with the water stored in the artificial basin. The results showed that, with proper choice of the value assigned to μ_0, the model allowed obtaining the desired degree of accuracy in predicting maximum wave run-up along with a significant reduction of the computational time.

An ongoing research is devoted to the application of SPHERA v.9.0.0 to the simulation of the post-failure dynamics of rainfall-induced shallow landslides that represents one of the most common natural hazards in some areas of the world (Bordoni et al. 20015). These kind of landslides are triggered by intense rainfall events inducing water infiltration at slopes that increases the volumetric water content and pore water pressure that worsen the slope stability. Therefore, reliable assessment of landslide susceptibility requires proper definition of the rainfall characteristics considering recent climate trends affecting rainfall and intense storm events (Barbero et al. 2014).

SPHERA v.9.0.0 is particularly suitable for the analysis of the above-mentioned kind of shallow landslides that are classified as complex landslides because their run-out starts as shallow rotational-translational failure then it changes into earth flows owing to the large water content and behaves like dense granular flow (Zizioli et al. 2013).

The early results of these simulation are shown and discussed in section 3.2.

3 RESULTS ANALYSIS

This section illustrates some applications of the two WCSPH models described in sections 2.1 and 2.2.

Section 3.1 shows the application of the standard SPH model for the analysis of multiphase flow involving two fluids with high-density ratio, as the case of a circular bubble rising in water at rest.

Section 3.2 is devoted to the application of the FOSS code SPHERA v.9.0.0 (Amicarelli et al. subm.) to the analysis of multiphase flow involving a viscous non-Newtonian fluid, as the case of post-failure dynamics of a rainfall induced shallow landslide.

3.1 Bubble rise in still water

The WCSPH model described in section 2.1 has been applied to the analysis of the problem investigated in Colagrossi & Landrini (2003). The free rise of a circular air bubble with radius r inside a still water column with depth H is simulated.

As said in the section 1, no additional term is included in the momentum balance equations

to account for surface tension effects. However, Colagrossi & Landrini (2003) and Hoover (1998) noticed that the discretized form of pressure gradient in the standard SPH momentum balance equation implies fictitious surface-tension effects. The adopted formulation of the momentum balance Eq. (11) maintains the same structure of standard SPH momentum balance equation because it is obtained through the same discretization procedure.

Table 1: model parameters for test case of rising bubble in water at rest. Superscripts refer to *w*=water *a*=air.

parameter	value
δ	0.025 m
h	1.3 δ
water	45,488 part.ls
air	2,512 part.ls
H	10 m
r	1 m
γ^w	7.0
γ^a	7.0
ρ^w	1000 kg/m^3
ρ^a	1.2 kg/m^3
c^w	50 m/s
c^a	55 m/s
ϑ	0.4
α_M	0.075

Table 1 summarizes the model parameters adopted in the computation. After early trial simulations, the optimal inter-particle distance δ = 0.025 m is adopted, resulting in 48,000 total particles. This resolution represents a suitable compromise between required computational effort and results quality. The air sound speed c^a has been properly reduced to a value close to the water sound speed c^w in order to enhance bubble deformation. In Table 1 ϑ is the constant for periodic density smoothing, α_M is the constant of Monaghan artificial viscosity.

Figure 1(a) displays the initial state of the half system that has been simulated to reduce the computational effort. The left-hand panel shows the velocity modulus, which is expressed in non-dimensional form with respect to the reference velocity $(g\,r)^{0.5}$. The mid panel displays the hydrostatic pressure distribution in the water column and the atmospheric (relative) pressure inside the bubble, both of which are expressed in non-dimensional form with respect to the pressure at the bottom of the tank ($\rho^w g\,H$). The right panel shows the density field. Note that the air particles are surrounded by a black circle in the left-hand and in the middle panels in order to distinguish them from the water particles. For this reason, air particles appear darker in the plots showing velocity magnitude and pressure distribution.

As the computation starts, the air bubble is suddenly compressed because of the strong pressure difference with respect to the surrounding water. Figure 1(b) shows the system at the instant at t = 0.70 s. The bubble assumes a lenticular shape because it is pushed upward by the water jet that rises from the bottom in the direction of the bubble vertical axis because of the pressure difference with respect to the air. The left panel shows the above-mentioned water jet

with a vertical velocity of about 4 m/s.

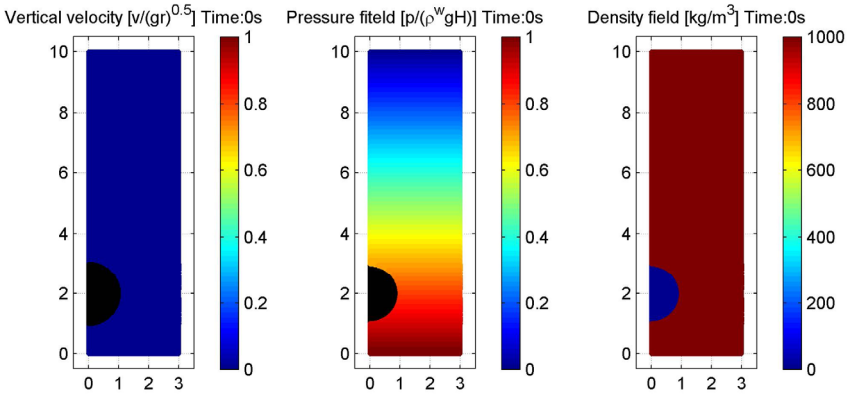

(a)

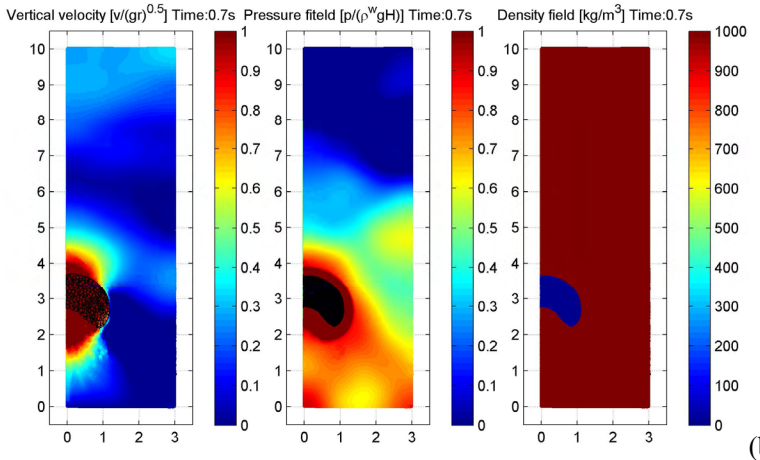

(b)

Figure 1: bubble rise at (a) t = 0.0s and (b) t = 0.70s. From the left-hand side: velocity, pressure and density fields. Cartesian axes in meters.

As seen in the middle panel, the water pressure is higher around the air bubble, causing it to become deformed during the upward motion. Both the velocity and pressure fields are quite smooth and vary in accordance with physical expectations.

The right-hand panel shows that the bubble contour remains quite regular, without penetration of water particles, thus highlighting fictitious surface tension effects even if the momentum balance equations does not include any term simulating physical surface tension. Owing to the hydrodynamic thrust of the upward water jet, the bubble vertical position increases, the bubble mean thickness decreases while the transversal length grows with respect to the early situation in Figure 1(b).

The bubble contour at time t = 1.40 s is shown in Figure 2 (red dots), and it is compared with the numerical result in the paper by Colagrossi & Landrini (2003), denoted by blue diamonds. It can be seen that the simulated bubble is characterized by a reduced vertical velocity and that its shape is rather different because the lower volute that subsequently

detaches from the upper main body does not form.

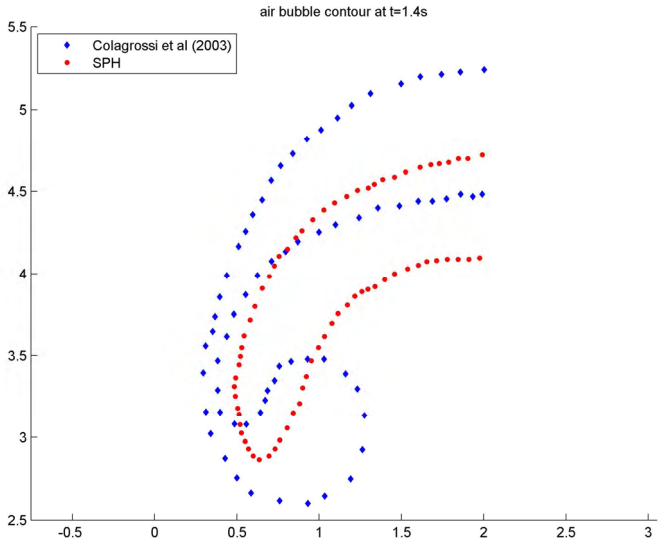

Figure 2: bubble position at t = 1.40 s. Comparison between present SPH model (red dots) and the model by Colagrossi & Landrini (2003).

Concerning the reduced rising speed of the air bubble, this may be related partly to the high dissipation effects induced by the artificial viscosity when both phases are compressed one to each other, as discussed in Manenti (2018).

Regarding the differences of the shape with respect to the reference results in Colagrossi & Landrini (2003), may be these are related to the fact that the present model does not implement any term for simulating physical surface tension effects in the momentum balance equation. Anyway, the adopted discretized form of the pressure gradient term implies fictitious surface-tension effects (Hoover, 1998) and this is partly confirmed by the inter-phase surface sharpness without heterogeneous particles penetration.

A similar problem was investigated in Sussman et al. (1994) considering a rising air bubble in a liquid with density ratio 1000/1, medium range Reynolds number and non-negligible surface tension effects (i.e. low Bond number). Qualitative comparison of the bubble shape shows that the results obtained with the present model are consistent with those of Sussman et al. (1994) showing that no fragmentation of the air bubble occurs even at subsequent instants. Anyway, a rigorous comparison is rather difficult owing to the following reasons. The governing equations for slightly compressible fluids are assumed in this model, while incompressible Navier-Stokes equations have been adopted in Sussman et al. (1994). The physical viscosity is neglected in the present model, and therefore it seems difficult to evaluate the Reynolds number based on the artificial viscosity contribution. The fictitious surface tension can not be easily quantified to estimate an equivalent physical surface tension for evaluating Bond number.

3.2 Rainfall induced shallow landslide

The FOSS code SPHERA v.9.0.0 (Amicarelli et al. subm.) illustrated in section 2.2 has

been tested for the post-failure analysis of a rainfall induced shallow landslide. This landslide occurred during an intense rainfall event on April 2009 in a hilly area of the Oltrepò Pavese named Recoaro valley – Northern Italy. Even if SPHERA has 3D formulation, a 2D approach has been conveniently adopted in this case because of the landslide peculiarity to be relatively narrow so as the flow may be assumed two-dimensional.

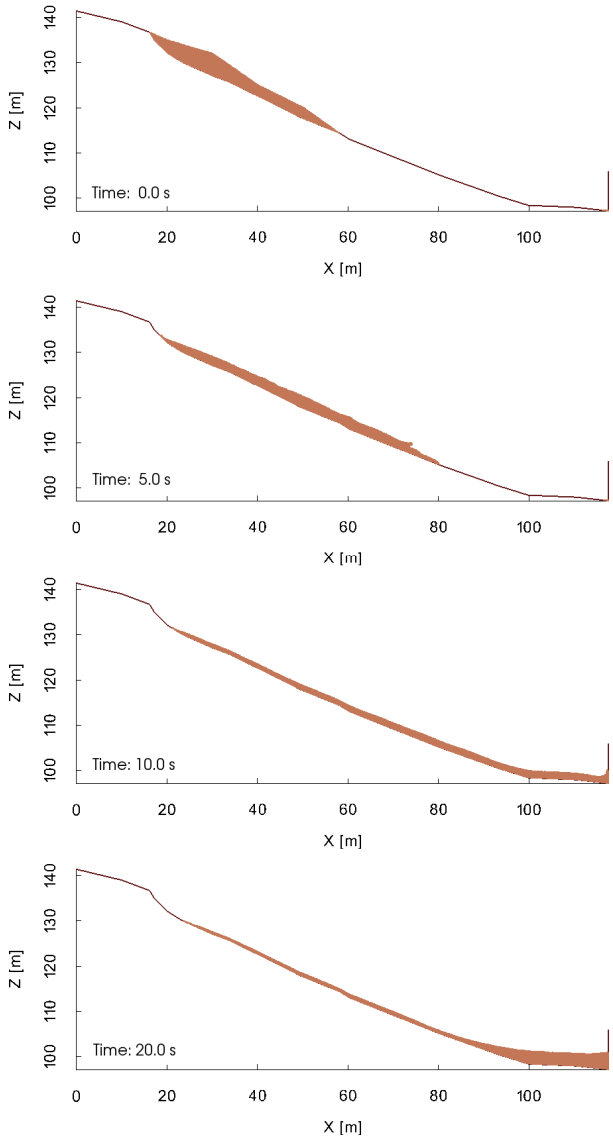

Figure 3: 2D SPH simulation of a rainfall induced shallow landslide. SPHERA v.9.0.0 (RSE SpA).

One of the first contribution to SPH modelling for predicting flow-like landslides including hydro-mechanical coupling was given by Pastor et al. (2009). They proposed a 2D depth-integrated, coupled, SPH model by assuming that the vertical flow structure would be the same as a uniform steady-state flow according to the so-called model of the infinite landslide having constant depth and moving at constant velocity on a constant slope. This assumption is

suitable for landslides whose average depths are small in comparison to their length and width.

In the present case, where initial landslide mean depth is of the same order of its length and width, significant variations of the vertical thickness and of the vertical velocity profile may occur along the landslide body in the flow direction. The proposed modelling approaches removes the hypothesis made by Pastor et al. (2009), thus allowing a numerical implementation of the problem that is closer to the actual behavior. The simulated falling time seems quite reasonable for the considered event. Comparison of the final landslide profile with in situ measurements shows suitable accuracy and will be illustrated in a future paper.

4 CONCLUSIONS

- A novel WCSPH based on standard formulation has been illustrated for the analysis of multiphase flows with large density ratio. By replacing the density (which is discontinuous at the interface) with specific volume, the numerical instability at the interface is prevented. Furthermore, no fictitious force should be added in the pressure gradient term inside the momentum balance equation to prevent interphase particle penetration and maintain the interface sharply defined. Kernel truncation is avoided at interface, thus reducing deterioration of computational accuracy.
- The FOSS code SPHERA v.9.0.0 (RSE SpA) was tested on the simulation of a rainfall induced shallow landslide occurred in Italy in 2009. The model, having full 3D formulation, allows removing the need for a depth integrated formulation. Fast computation is assured by introducing a numerical parameter, the limiting viscosity, for run optimization.

ACKNOWLEDGMENTS

We acknowledge the CINECA award under the ISCRA initiative for the availability of high performance computing resources and support. HPC simulations on SPHERA refer to the following HPC research project: HPCNHLW1—High Performance Computing for the SPH Analysis of Natural Hazard related to Landslide and Water interaction (Italian National HPC Research Project); instrumental funding based on competitive calls (ISCRA-C project at CINECA, Italy); 2019; S. Manenti (Principal Investigator) et al.; 360,000 core-hours.
The work in sect. 3.2 has been supported by Fondazione Cariplo, grant n°2017-0677.

REFERENCES

[1] Amicarelli A., S. Manenti, R. Albano, G. Agate, M. Paggi, L. Longoni, D. Mirauda, L. Ziane, G. Viccione, S. Todeschini, A. Sole, L.M. Baldini, D. Brambilla, M. Papini, M.C. Khellaf, B. Tagliafierro, L. Sarno, G. Pirovano. Submitted to Computer Physics Communications; "SPHERA v.9.0.0: a Computational Fluid Dynamics research code, based on the Smoothed Particle Hydrodynamics mesh-less method".

[2] Amicarelli A., Kocak B., Sibilla S., Grabe, J. "A 3D smoothed particle hydrodynamics model for erosional dam-break floods" *Int. J. Comput. Fluid Dyn*. 31(10), 413–434, 2017. https://doi.org/10.1080/10618562.2017.1422731.

[3] Barbero G., Moisello U., Todeschini S. "Evaluation of the areal reduction factor in an urban area through rainfall records of limited length: a case study". *J. of Hydrologic*

Eng. (ASCE), (2014) 19(11): 05014016-1-10.
[4] Bordoni M., Meisina C., Valentino R., Bittelli M., Chersich S. "Site-specific to local-scale shallow landslides triggering zones assessment using TRIGRS". *Nat. Hazards Earth Syst. Sci.*, (2015) 15: 1025–1050 doi:10.5194/nhess-15-1025-2015.
[5] Ciaponi C., Murari E., Todeschini S. "Modularity-Based Procedure for Partitioning Water Distribution Systems into Independent Districts". *Water Resources Management*, (2016) 30(6): 2021-2036, doi:10.1007/s11269-016-1266-1.
[6] Colagrossi A., Landrini M. "Numerical simulation of interfacial flows by smoothed particle hydrodynamics". *J. Comp. Phy*. (2003) 191, pp: 448–475.
[7] Domínguez J. M., Crespo A. J. C., Gómez-Gesteira M. "Optimization strategies for CPU and GPU implementations of a smoothed particle hydrodynamics method," Comput. Phys. Commun. (2013) 184(3): 617-627.
[8] Grenier N., Antuono M., Colagrossi A., Le Touzé D., Alessandrini B. "An Hamiltonian interface SPH formulation for multi-fluid and free-surface flows(2009). *J. Comp. Phy*. (2009) 228, pp: 380-393.
[9] Guandalini R., Agate G., Manenti S., Sibilla S., Gallati M. "SPH Based Approach toward the Simulation of Non-cohesive Sediment Removal by an Innovative Technique Using a Controlled Sequence of Underwater Micro-explosions". *Procedia IUTAM*, (2015) 18, 28–39.
[10] Guandalini R., Agate G., Manenti S., Sibilla S., Gallati M. "Innovative numerical modeling to investigate local scouring problems induced by fluvial structures". *Proc. 6th Int. Conf. on Bridge Maintenance, Safety and Management* (IABMAS 2012), Stresa, Lake Maggiore, Italy, 8–12 July 2012; pp. 3110–3116, 2012.
[11] Hoover W.G. "Isomorphism linking smooth particles and embedded atoms". *Physica* A 260 (1998) 244–254.
[12] Hu X.Y., Adams N.A. "An incompressible multi-phase SPH method". *J. Comp. Phy*. (2007) 227, pp:264–278.
[13] Liu G.R. & Liu M.B. *Smoothed Particle Hydrodynamics – a meshfree particle method*. (2003) World Scientific.
[14] Manenti S., Wang D., Domínguez J.M, Li S., Amicarelli A., Albano R. Submitted to *Water*: "SPH modelling of water-related natural hazards".
[15] Manenti, S. "Standard WCSPH for free-surface multi-phase flows with a large density ratio". *Int. J. of Ocean and Coastal Eng.* - Vol. 1, No. 2 (2018) 1840001 (39 pages) World Scientific Publishing Company. DOI: 10.1142/S2529807018400018.
[16] Manenti, S., Amicarelli, A., Todeschini, S. "WCSPH with Limiting Viscosity for Modeling Landslide Hazard at the Slopes of Artificial Reservoir". *Water*, (2018) 10(4), 515; doi:10.3390/w10040515
[17] Manenti S., Pierobon E., Gallati M., Sibilla S., D'Alpaos L., Macchi E., Todeschini S. "Vajont Disaster: Smoothed Particle Hydrodynamics Modeling of the Postevent 2D Experiments". *J. Hydraul. Eng.*, (2016) 142, 05015007.
[18] Manenti S., Sibilla S., Gallati M., Agate G., Guandalini R. "SPH Simulation of Sediment Flushing Induced by a Rapid Water Flow". *J. of Hydr. Eng.* 2012, Vol. 138, No. 3, pp. 272-284, March 1 (2012) ISSN 0733-9429/2012/3-0–0 DOI:10.1061/(ASCE)HY.1943-7900.0000516.
[19] Monaghan J.J., Ashkan R. "A simple SPH algorithm for multi-fluid flow with high

density ratios". *Int. J. Numer. Meth. Fluids* (2013) 71:537–561.
[20] Monaghan, J. J. "Simulating free surface flows with SPH". *J. Comp. Physics*, (1994) 110(2), pp. 399–406.
[21] Newman J.P., Maier H.R., Riddell G.A. et al. "Review of literature on decision support systems for natural hazard risk reduction: Current status and future research directions". *Environmental Modelling & Software* (2017) 96, 378-409.
[22] Pastor M., Haddad B., Sorbino G., Cuomo S., Drempetic V. "A depth-integrated, coupled SPH model for flow-like landslides and related phenomena". *Int. J. Numer. Anal. Methods Geomech*. 2009, 33, 143–172. https://doi.org/10.1002/nag.705 .
[23] SPHERA v.9.0.0 (RSE SpA). https://github.com/AndreaAmicarelliRSE/SPHERA
[24] Sussman M., Smereka P., Osher S. "A level set approach for computing solutions to
[25] Todeschini S., Manenti S., Creaco E. "Testing an innovative first flush identification methodology against field data from an Italian catchment". *J. of Environmental Management*, (2019) 246: 418-425, doi:10.1016/j.jenvman.2019.06.007.
[26] Zizioli D., Meisina C., Valentino R., Montrasio L. "Comparison between different approaches to modeling shallow landslide susceptibility: a case history in Oltrepo Pavese, Northern Italy". *Nat. Hazards Earth Syst. Sci.*, 13, 559–573, 2013. doi:10.5194/nhess-13-559-2013.